

Structural features of hydrogenated E110opt and E635 tubes

M. G. Isaenkova, Professor¹, Doctor of Physical and Mathematical Sciences, e-mail: MGIsaenkova@mephi.ru

M. I. Petrov, Engineer¹, e-mail: mipetrov.99@yandex.ru

I. V. Kozlov, Engineer¹, e-mail: ilya_mephist@mail.ru

A. V. Bogomolova, Engineer¹, e-mail: bogomolova@m-a-l.ru

¹National Research Nuclear University "MEPhI"

The paper investigates the behavior of the hydride phase in hydrogenated tubes made of Russian zirconium E635 and E110opt alloys. The orientation and fraction of mesoscale hydrides in the alloy matrix have been described by analyzing optical metallographic images using the developed software. Metallographic images were used to assess the predominant orientation of hydrides in the axial section of the tube, as well as the surface density of the hydride phase with an increase in the concentration of hydrogen in tubes made of different alloys. It has been shown that increasing the hydrogen concentration to 600–700 wppm increases the number of radially oriented hydrides, which is associated with the development of compressive radial stress during the formation of tangentially oriented hydrides at the initial stage. Increasing the hydrogen concentration in E110opt alloy cladding tubes to 600–700 wppm leads to a change in the orientation of the α -zirconium basal axes, which results in an increase in the integral textural f_R -parameter and a decrease in the f_T - and f_L -parameters. This change is due to the development of radial compressive stress and is only possible due to the activation of twinning in the grains, the basal axes of which are deflected from the compressive stress at an angle of up to 90 degrees.

The results of synchrotron Debye rings and X-ray reflection diffraction analysis revealed patterns of structure and texture formation of zirconium matrix and hydrides with increasing hydrogen concentration in E110opt and E635 tube materials. Twinning by the $\{10\bar{1}2\}\langle 10\bar{1}1 \rangle$ and $\{10\bar{1}1\}\langle 10\bar{1}2 \rangle$ systems has been detected in the alloy E110opt. It reorients the basal axes at angles of 85° and 57.2° in the direction of compressive stress applied in the radial direction. According to the crystal lattice geometry of the α -phase, this reorientation occurs in the direction deviated from the radial direction by 30 degrees. It has been established that in E635 alloy hydrides with $\{001\}\langle 110 \rangle$ orientation are predominantly formed, but hydrides with additional $\{110\}\langle 011 \rangle$ and $\{110\}\langle 112 \rangle$ orientations are also present in smaller amounts. In the E110opt alloy there are hydrides of $\{001\}\langle 110 \rangle$ and $\{110\}\langle 011 \rangle$ orientations as well as $\langle 112 \rangle$ in approximately equal proportions. The presence of hydrides with a $\langle 112 \rangle$ partially axial textural component is due to activation in the α -phase of twinning along the $\{10\bar{1}2\}$ and $\{10\bar{1}1\}$ planes, in which hydrides are formed according to the established orientation relationship $(0001)_{\alpha-Zr} \parallel \{111\}_{\delta-ZrH_{1.66}}$.

Key words: zirconium alloys, hydrides orientation, microstructure, crystallographic texture, X-ray, synchrotron radiation, orientation relationship.

DOI: 10.17580/nfm.2023.01.07

1. Introduction

Zirconium alloys combine high mechanical properties, corrosion resistance, and low neutron absorption cross-section [1–4]. Therefore, they are used for the manufacture of structural elements and nuclear fuel cladding of the core of VVER nuclear reactors. Hydrogen is among the causes of embrittlement of structural materials in modern nuclear reactors, leading to reduction of service life of their structural elements [5–8]. In the nuclear reactor core, fuel elements such as the fuel rod cladding, spacer grids, angles, guide channels, and so on are exposed to thermal and mechanical stress that can cause deformation of components, neutron flux that causes radiation damage, and chemical effects of coolant that lead to material corrosion and hydrogenation.

Zr alloys oxidize slowly and uniformly due to the reaction of the outer surface of the product material with cooling water. This produces a corrosion protection layer consisting mainly of monocline zirconium dioxide,

according to the reaction: $Zr + 2H_2O = ZrO_2 + 2H_2$ [9–10]. The source of hydrogen which is of most concern is the trapping of hydrogen by the zirconium alloy cladding during this reaction. As argued in [11], only hydrogen from corrosion enters the cladding, although there are other sources of hydrogen (e.g., radiolysis of water). When the content of hydrogen dissolved in Zr alloys exceeds its solubility limit in the solid state, zirconium hydrides precipitate as lenticular plates [7–12]. Hydride formation can significantly degrade mechanical properties of the materials, which leads to a decrease in both ductility and fracture toughness [13–19].

One manifestation of the influence of hydrogen on the behavior of zirconium products, especially channel tubes made of Zr – 2.5% Nb alloy, is the delayed hydride cracking (DHC) developing under cyclic loading conditions and described in detail in papers [20–21]. At the same time, hydride cracking of cladding tubes during their operation for 2.5–3 years did not occur. However, at present,

due to the increase in the service life of fuel rods from three to five years and subsequent transportation and storage of spent fuel, the relevance of the hydride topic is also increasing. Fuel burnup and, consequently, neutron fluence and increased hydrogen concentration in the material are increasing, which leads to changes in its microstructure, including an increase in the density of dislocation loops and the dissolution and re-emission of both intermetallic particles [22, 23] and hydrides. These microstructural changes can degrade the cladding tube characteristics due to variations in mechanical properties (hardening, embrittlement, loss of fracture toughness), dimensional variations associated with irradiation-induced deformation (creep and growth), and changes in corrosion resistance.

It is known [22, 23] that radiation damage-related hardening and embrittlement reach saturation after one month in the reactor. A potentially major concern is the corrosion of the cladding tube during interaction with reactor coolant water and the resulting hydrogen intrusion into the zirconium cladding (hydrogen pickup) that occurs during reactor operation.

It was shown in [24, 25] that the rate of DHC depends on the crystallographic texture and decreases linearly with increasing values of the f_R/f_T ratio in logarithmic coordinates regardless of the alloy composition and structure (as well as in the case of the yield strength), where f_R and f_T are integral Kearns textural parameters that characterize the projection of the basal axes of the grain structure to the external directions in the tube: radial R and tangential T .

The prospect of dry storage of spent fuel assemblies implies a long, well beyond service life, duration of zirconium alloy resistance to the harmful effects of hydrogen. An understanding of the mechanisms and patterns of hydride formation and growth during hydrogenation is necessary to assess the alloys' ability to resist this impact.

The foreign literature presents a great number of studies on the structure and morphology of hydride phases [9, 10, 26–39], their orientation depending on the crystallographic texture, as well as reorientation under the influence of external stress. However, most of the studies were carried out for products made of alloys of Zircaloy or Zr – 2.5% Nb, annealed after 20% cold rolling at 400 °C for 24 hours (according to the technology for obtaining tubes for the CANDU reactor). Russian alloys differ significantly in both structure and properties, which predetermines their differences with respect to hydride formation [40, 41]. Thus, the study [41] demonstrated a difference in the enthalpy of hydride formation in the E110opt and E635 alloys. The results of differential scanning calorimetry showed that E110opt alloy has higher value of enthalpy of hydride precipitation ΔH_p compared to other alloys such as Excel and Zircaloy-4. E635 alloy is close to the foreign Zircaloy-4 alloy by this parameter and both of them are higher than in Excel and Zr-2.5Nb alloys in which the problem of DHC has been most acute [9, 20, 21].

In [40] it has been shown that in the E110 alloy shorter hydrides are formed compared to the Zircaloy-4 and

Zr – 2.5% Nb alloys, which may also be associated with a higher value of the enthalpy of hydride precipitation ΔH_p , and that for the Zircaloy-4 and Zr – 2.5Nb one orientation relationship $(0001)_{\alpha-Zr} \parallel \{111\}_{\delta-ZrH_{1.66}}$ is performed, and for the Zr – 1 Nb (E110) alloy in addition to the indicated for about half of the grains the relationship $(0001)_{\alpha-Zr} \parallel \{100\}_{\delta-ZrH_{1.66}}$ is performed. The presence of tension twins $\{10\bar{1}2\}\langle 10\bar{1}1\rangle$ and compression twins $\{10\bar{1}1\}\langle 10\bar{1}2\rangle$ in alloy E110, which were not observed in alloy Zircaloy-4 and Zr-2.5Nb has also been noticed in the paper.

Therefore, the purpose of this study is to organize the numerous data and identify the main patterns of structure changes in E635 and E110opt Russian alloys when the hydrogen concentration increases in the absence of external stress.

2. Samples and methods of their investigation

The study was carried out on the tubes of length (35 ± 1) mm which were cut from the fuel cladding with diameter $\varnothing 9.1 \times 7.93$ mm of E110opt alloy (Zr – 1 Nb – 0.06 Fe – 0.08 O, wt.%) characterized by complete recrystallization of material, and guide channel $\varnothing 12.6 \times 10.9$ mm from alloy E635 (Zr – 1 Nb – 1.2 Sn – 0.35 Fe – 0.08 O, wt.%), being in partial recrystallized state. The samples were saturated with hydrogen to concentrations of 40 to 700 wt ppm by hydrogenation from the gas phase at a fixed temperature in the range of 400–550 °C, depending on the calculated hydrogen concentration. After hydrogenation, the actually achieved hydrogen concentrations were measured with LECO for two 2 mm high rings cut from the top and bottom of the branch tube. The average value of the hydrogen concentrations measured for the two rings is used further as the concentration for the branch tube in question.

The following research methods have been used in this study: metallographic analysis, X-ray diffraction phase analysis and analysis of the structural state of phases by X-ray line profile [42], textural analysis by diffractometric imaging [43–45] and Debye rings obtained by transmission of 120–150 μm thick foil at synchrotron radiation [46–47]. Different cross sections of hydrogenated tubes were fabricated for the methods used. The sections are further denoted by the name of the normals to their plane, parallel to the main directions in the tube: R – radial; T – tangential; L – longitudinal or axial.

So, for metallographic analysis, 4 mm high rings were cut using precision electrospark cutting with 200 μm thick wire. Samples have been cut into two semi-rings strictly along the diameter to obtain a section perpendicular to the tangential direction, i.e., a T -section. The second half-ring has been used to prepare an L -section perpendicular to the longitudinal direction of the tube.

The microstructure of the samples has been examined using a MIM-7 metallographic microscope. In the Russian literature, the coefficient F_n [1], equal to the ratio of the total length of the hydrides forming an angle less than 45° with the radial direction to the total length of all

hydrides, is used to describe the pattern of preferential orientation of the hydrides. In foreign literature, the *RHC* coefficient is used as such a parameter [10, 19], for the calculation of which hydrides are divided into 3 categories according to the angle they form with the tangential direction: “in-plane” (in-plane hydrides coefficient – *IHC*) – $(0 \div 40)^\circ$, “out-of-plane” (*OHC*) – $(65 \div 90)^\circ$ and “mixed” (*MHC*) – $(40 \div 65)^\circ$. For each of the categories, the ratio of hydrides normalized to length is determined. Thus, the *RHC* coefficient is:

$$RHC = 0.5 \cdot MHC + OHC.$$

Using the developed software, the metallographic images were analyzed, which resulted in the calculation of F_n and *RHC* coefficients describing the preferential orientation of hydrides.

The errors were estimated as follows: each image was divided into 4 fragments and the hydride orientation coefficients F_n and *RHC* described above were calculated for each fragment. The difference in the results is due to the heterogeneity of the hydride distribution over the cross section of the sample, as well as to the fact that the determination of the tube contours is associated with the error arising from the approximation of the tube contours by arcs of circles. The coefficient measurement error is $\delta(F_n) = 24\%$ and $\delta(RHC) = 28\%$.

X-ray analysis of the structure and texture of the zirconium matrix and hydride phases was performed using synchrotron radiation with a wavelength of 0.74 Å and filtered copper radiation with a wavelength of 1.54 Å. Synchrotron studies were carried out at the “KISI-Kurchatov” facility. The transmission imaging of thin rings of 100–120 μm thickness was used. Registration of Debye rings was carried out on a 2D-detector. The summation of intensity of reflection along a circle allows to carry out quantitative phase analysis. Moreover, it is possible to reconstruct direct pole figures (DPF) for all phases presented in the material by the registered Debye rings [44]. Conventional *X*-ray structure and texture analysis of the samples has been performed on D8 Discover, DRON-3 and DRON-3M *X*-ray diffractometers using Cu K_α - and Cr K_α -radiation. Recording of diffraction spectra to determine the phase composition of the samples and assess their structural state has been carried out on a Bruker D8 Discover diffractometer using Cu K_α -radiation and a position-sensitive LynxEye detector. The imaging was performed with a step of 0.01° Bragg angle of 2θ and an accumulation of 0.5 s per detector strip, which gives a total of about 96 s per point. The BrukerAXS DIFFRAC.EVA v.4.2 software and the international ICDD PDF-2 database were used for phase identification.

The crystallographic texture has been determined from the DPFs. The initial incomplete DPFs were used to reconstruct the orientation distribution function (ODF) [45, 46] with subsequent construction of full DPF(0001) and calculation of the integral Kearns parameters for the hexagonal phase α -Zr.

3. Experimental results

3.1. Microstructure of hydrogenated zirconium tubes

Fig. 1 shows optical images for three mutually perpendicular tube sections (*R*, *T*, *L*) of a typical hydrogenated sample.

The metallographic images obtained for the *L*-section are used to estimate the hydride orientation with respect to the *R*- and *T*-directions. **Fig. 2** shows plots of the dependences of the F_n and *RHC* coefficients on the hydrogen content for the two alloys. The plots are approximated to a straight line by the Pearson method (χ^2 minimum), since the measurement errors differ for each point. The graphs show a linear increase in both coefficients, i.e., an increase in the number of hydrides oriented radially with increasing hydrogen concentration in the material.

3.2. *X*-ray phase analysis of the investigated tubes

Fig. 3 shows the change in *X*-ray spectra recorded using synchrotron radiation. The spectra are recalculated to the wavelength of copper radiation for the convenience of subsequent comparison with the diffraction spectra obtained on the copper radiation of the *X*-ray diffractometer.

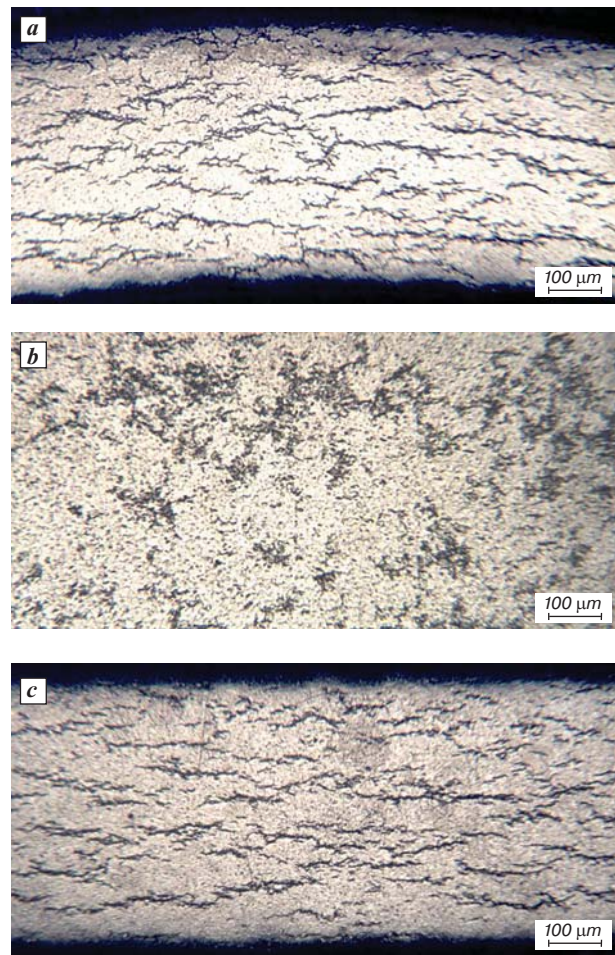


Fig. 1. Metallographic structure of alloy E110 opt with 250 wppm hydrogen content:
a – *L*-section, b – *R*-section, c – *T*-section

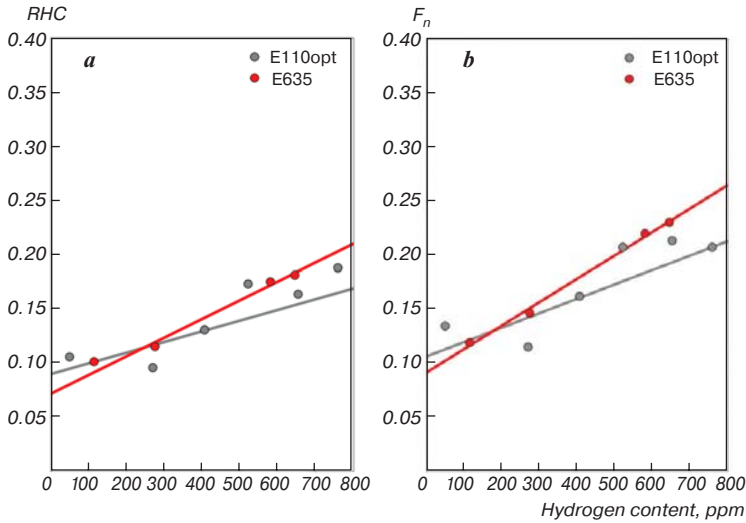


Fig. 2. Dependences of RHC (a) and F_n (b) coefficients for E110opt and E635 alloys on hydrogen content

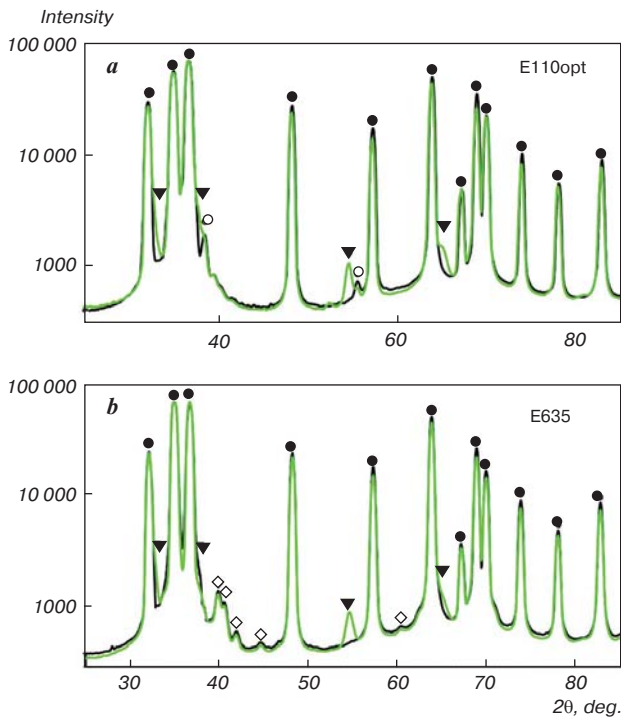


Fig. 3. X-ray diffraction patterns for hydrogenated tubes made of E110opt (0 ppm – black, 320 ppm – green) (a) and E635 (0 – black, 400 ppm – green) (b) alloys obtained by transmission of 120 μm thick rings. Dots of different shapes mark the positions of the peaks.
 ● – α -Zr; ○ – β -Nb; ◇ – Laves phase and ▼ – δ -hydride $\text{ZrH}_{1.66}$

In the case of recording Debye rings on synchrotron radiation, the intensity along them is summed, so the presented spectra are not influenced by the texture. Using synchrotron radiation also substantially increases the intensity of reflections from additional phases thereby increasing the sensitivity of the analysis to these phases. Identification of weak lines from additional phases is more clear when using a logarithmic scale of the intensity of reflections for the ordinate axis.

Fig. 3 clearly shows the peaks of additional phases: β -phase for E110-alloy and intermetallic phase $\text{Zr}(\text{Nb},\text{Fe})_2$ for E635 alloy. The observed broadening of the X-ray lines around their base and the appearance of new maximums allow us to unambiguously identify δ -hydride phase ($\text{ZrH}_{1.66}$), which, as can be seen from the spectrum, is the only hydride modification in the studied samples.

3.3. Analysis of crystallographic texture

Based on the results of the crystallographic texture analysis for tubes made of different alloys saturated with hydrogen to different concentrations, plots of changes in the ratio of integral texture parameters f_R/f_T for different hydrogen content in the product have been constructed.

According to the results shown in Fig. 4, the tubes made of E635 alloy have no changes in the distribution of basal axes, while in the E110 alloy there is a reorientation of basal axes from the tangential to the radial direction, i.e. the number of grains whose basal axes are oriented close to the radial direction increases. Such reorientation is possible only in the case of tensile stress acting in the tangential direction as a result of the formation of a large number of hydrides oriented circumferentially. In particular, when hydrides are formed, the material is compressed along the c -direction. Since the total volume does not change, tensile stress must be observed in the T - and L - directions. Relaxation of such stress occurs either by changing the orientation of the hydrides or by the development of twinning. For E110 alloy, as will be shown below, twinning is observed, while in E635 alloy it is suppressed.

Fig. 5 shows the DPFs (0001) for α -zirconium and $\{111\}$ for δ -hydride for L -section based on the Debye rings obtained with synchrotron radiation.

According to the data obtained (Fig. 5), the texture components of δ -hydride in E635 alloy tubes are the main one $\{001\}\langle 110 \rangle$ and additional ones are $\{110\}\langle 011 \rangle$ and $\{110\}\langle 112 \rangle$. The hydrides with orientations $\{001\}\langle 110 \rangle$ and $\{110\}\langle 011 \rangle$, as well as $\langle 112 \rangle$ are present in approximately equal proportions in E110opt alloy tubes. The presence of hydrides with the partially axial textural component $\langle 112 \rangle$ (extended textural maximum is present in the region of maximum compressive stress along the radial direction) is caused by activation of twinning along the planes $\{10\bar{1}2\}$ and $\{10\bar{1}1\}$ in the α -phase [49], in which hydrides are formed according to the established orientation relationship $(0001)_{\alpha\text{-Zr}} \parallel \{111\}_{\delta\text{-ZrH}_{1.66}}$.

4. Discussion of the results

4.1. Hydride orientation change with increasing hydrogen concentration in the material

The increase in the fraction of radially oriented hydrides with increasing hydrogen content (Fig. 2) seems to be due to the appearance of compressive stress in

the radial direction during the formation of hydrides oriented in the tangential direction. As a consequence, tensile stresses develop in the T -direction, and, as we know, since hydride formation is associated with an increase in

volume, the growth of mesoscale hydrides occurs in the direction perpendicular to the tensile stress, thereby relaxing stress. Therefore, the probability of radial hydrides increases.

The development of radial compressive stress during hydride formation in hydrogenated tubes is also indicated by a decrease in the distance between the basal planes with increasing hydrogen concentration (Fig. 4, b).

4.2. Crystallographic texture α -Zr and hydride phase

Analysis of the dependences of the Kearns integral texture parameters on the hydrogen content in the alloys (Fig. 4, a) allows us to conclude that the basal axes of the grains oriented in the T - and L -directions are reoriented toward the R -direction, i. e. along the compressive stresses acting in the radial direction. This suggests that the hydride nucleation in the E110opt alloy accompanied by deformation of the zirconium matrix leads to the twinning detected in the DPF(0001) analysis (Fig. 5). At the same time, this effect is not observed in the E635 alloy, or at least is observed on a smaller scale,

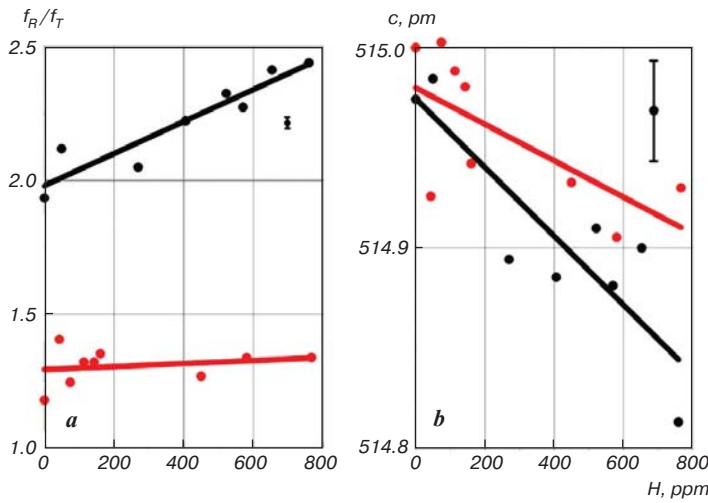


Fig. 4. Dependences of the f_R/f_T and α -Zr lattice parameter c for middle layers of E110 (black) and E635 (red) tubes on hydrogen concentration

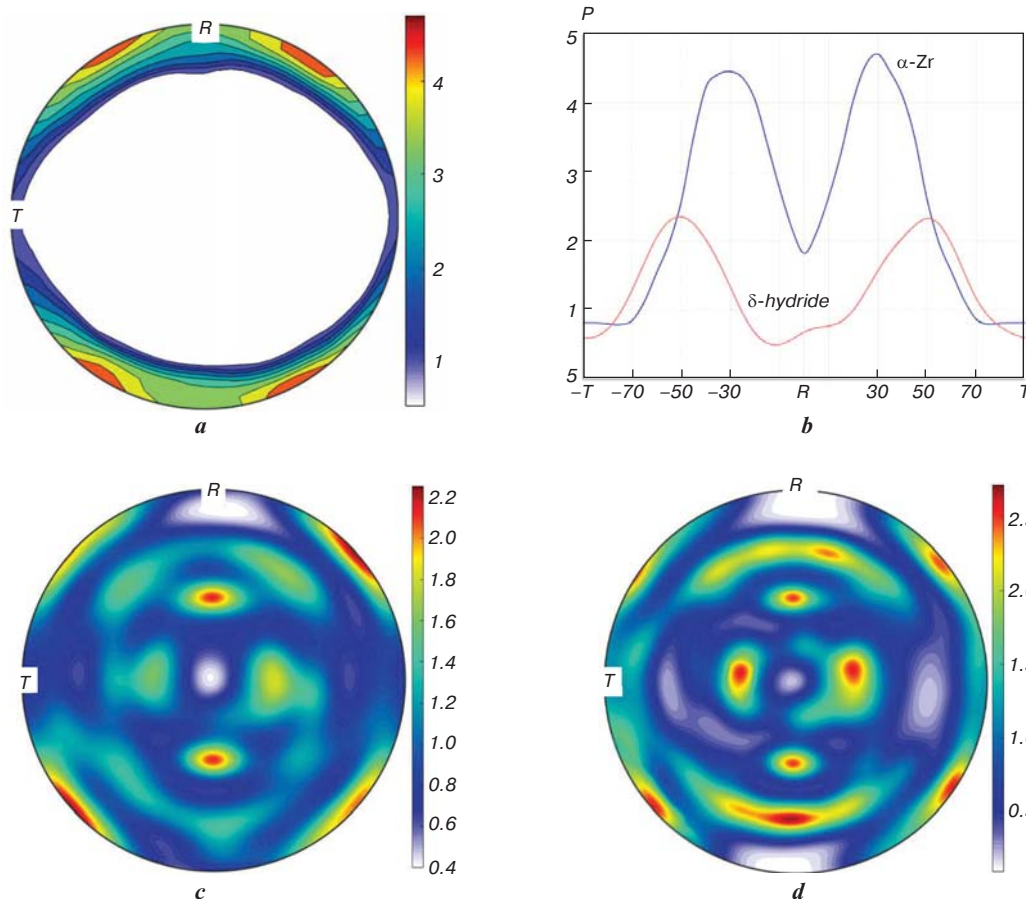


Fig. 5. $DPF(0001)_\alpha$ (a) and $\{111\}_\delta$ (c, d) for the L -section of a E110opt tube without hydrogen (a), as well as hydrogenated E635 (600 ppm) (c) and E110opt (700 ppm) (d) tubes; the distributions of the α -Zr basal axes and δ -hydride $\langle 111 \rangle$ axes in the R - T -section (b)

which may be due to the higher yield strength of the alloy to activate twinning preventing changes in the volume of α -matrix during hydride precipitation and twin formation.

As shown in 3.3, due to the orientation relationship performed during hydride formation as well as due to the features of their separation at the grain boundaries [9–10], the radial preferential orientation of the basal axes contributes to favorable hydride orientation in the tube and the tangential orientation contributes to unfavorable orientation. Thus, the observed grain reorientation pattern in the E110opt alloy indicates an increase in its resistance to hydride reorientation in the field of tensile tangential stresses during thermal cycles with an increase in hydrogen content.

In [40] the orientation relationships between the α -matrix and delta-hydride for Zircaloy-4, Zr – 1 Nb and Zr – 2.5 Nb alloys were established. The results of this work confirm the basic orientation relationship $(0001)_{\alpha-Zr} \parallel \{111\}_{\delta-ZrH_{1.66}}$ for E110opt and E635 alloys. The results of texture analysis refute the presence of the mentioned additional orientation relationship $(0001)_{\alpha-Zr} \parallel \{100\}_{\delta-ZrH_{1.66}}$ and confirm the presence of twins $\{10\bar{1}2\}$ $\langle 10\bar{1}1 \rangle$ in E110opt alloy. This is evidenced by the presence of partially axial textural components $\langle 112 \rangle$ δ -hydride on *DPF* $\{111\}$ for alloy E110opt, formed by reorientation of α -Zr basal axes at 85° and 57.2° angles for the indicated twinning systems, respectively. Thus, it can be concluded that the twinning process contributes to the appearance of a new orientation of the hydride grains due to the reorientation of the basal axes, but not because of the presence of an additional orientation relationship, but because of the release of hydrides in the twinned regions of the α -zirconium matrix.

5. Conclusions

1. The dependences of the hydride orientation coefficients on the hydrogen concentration in tubes made of Russian zirconium alloys E110 opt and E635 are obtained. It was found that an increase in the hydrogen content in the range of 40–700 wppm contributes to an increase in the number of radial hydrides in both alloys. This is due to the appearance of compressive stresses in the radial direction during the formation of tangentially oriented primary hydrides. It should be noted that the fraction of radial hydrides increases faster in the E635 alloy than in the E110 alloy. This is probably due to easier stress relaxation in the E110 alloy.

2. In the E110opt alloy, with an increase in the amount of hydrogen (hydrides), an increase in the ratios of the parameters f_R/f_T and a decrease in the period c of the α -Zr crystal structure are observed, which indicates an increase in compressive stresses in the radial direction of the tubes. Also, with an increase in the hydrogen concentration, activation of twinning along the systems $\{10\bar{1}2\}\langle 10\bar{1}1 \rangle$ and $\{10\bar{1}1\}\langle 10\bar{1}2 \rangle$ is observed, reorienting the basal axes in the direction of compressive stresses at angles of 85° and 57.2° , respectively.

3. It has been established that hydrides with the $\{001\}$ $\langle 110 \rangle$ orientation are predominantly formed in the E635 alloy, but hydrides with additional orientations $\{110\}\langle 011 \rangle$ and $\{110\}\langle 112 \rangle$ are also present in a smaller amount. In the E110opt alloy, hydrides with orientations $\{001\}\langle 110 \rangle$ and $\{110\}\langle 011 \rangle$, as well as $\langle 112 \rangle$, are present in approximately equal proportions. The presence of hydrides with a partially axial texture component $\langle 112 \rangle$ (an extended texture maximum is present in the region of maximum compressive stresses along the radial direction) is due to the activation of twinning along the $\{10\bar{1}2\}$ and $\{10\bar{1}1\}$ planes in the α -phase, in which hydrides are formed according to with the established orientation relationship $(0001)_{\alpha-Zr} \parallel \{111\}_{\delta-ZrH_{1.66}}$.

Acknowledgments

The work was carried out with the financial support of the Russian Federation represented by the Ministry of Science and Higher Education of the Russian Federation (Agreement No. 075-15-2021-1352).

The authors are grateful for the provision of samples for research to the Joint-Stock Company “Advanced Research Institute of Inorganic Materials named after Academician A. A. Bochvar” and his employees Plyasov A. A. and Saburov N. S., as well as the employees of the National Research Nuclear University MEPhI Fesenko V. A. and Mikhalev N. A.

References

- Zaimovsky A. S., Nikulina A.V., Reshetnikov N. G. Zirconium Alloys in Nuclear Power Engineering. 2nd ed., rev. and suppl. Moscow: Energoatomizdat, 1994. 252 p.
- Douglass D. L. The Metallurgy of Zirconium. Transl. from Eng. Moscow: Atomizdat, 1975. 360 p.
- Lemaignan C., Motta A. T. Zirconium Alloys in Nuclear Applications. In: *Materials Science and Technology*. Weinheim, Germany: Wiley-VCH Verlag GmbH & Co. KGaA, 2006.
- Lee J. M., Hong S. I. Design and Mechanical Characterization of a Zr – Nb – O – P Alloy. *Materials and Design*. 2011. Vol. 32, Iss. 8-9. pp. 4270–4277.
- Delayed Hydride Cracking in Zirconium Alloys in Pressure Tube Nuclear Reactors: Final Report of a Coordinated Research Project 1998–2002. Vienna: International Atomic Energy Agency, 2004. 85 p.
- Delayed Hydride Cracking of Zirconium Alloy Fuel Cladding: IAEA Tecdoc Series No. 1649. Vienna: IAEA, 2010. 66 p.
- Tan J., Ying S., Li C., Sun C. Effect of Zirconium Hydrides on Cyclic Deformation Behavior of Zr – Sn – Nb Alloy. *Scripta Materialia*. 2006. Vol. 55, Iss. 6. pp. 513–516.
- Lee K. W., Hong S. I. Zirconium Hydrides and Their Effect on the Circumferential Mechanical Properties of Zr – Sn – Fe – Nb Tubes. *Journal of Alloys and Compounds*. 2002. Vol. 346, Iss. 1. pp. 302–307.
- Puls M. P. The Effect of Hydrogen and Hydrides on the Integrity of Zirconium Alloy Components. Delayed Hydride Cracking. London: Springer-Verlag, 2012. 475 p.

10. Motta A. T., Capolungo L., Chen L.-Q., Cinbiz M. N., Daymond M. R., Koss D. A., Lacroix E., Pastore G., Simon P.-C. A., Tonks M. R., Wirth B. D., Zikry M. A. Hydrogen in Zirconium Alloys: a Review. *Journal of Nuclear Materials*. 2019. Vol. 518. pp. 440–460.
11. B. Cox, C. Roy. The Use of Tritium as a Tracer in Studies of Hydrogen Uptake by Zirconium Alloys, vol. 2519, Atomic Energy of Canada Ltd., Chalk River Nuclear Laboratories AECL, 1965.
12. Chu H. C., Wu S. K., Kuo R. C. Hydride Reorientation in Zircaloy-4 Cladding. *Journal of Nuclear Materials*. 2008. Vol. 373, Iss. 1-3. pp. 319–327.
13. De Menibus A. H., Auzoux Q., Dieye Q., Berger P., Bosonnet S., Foy E., Macdonald V., Besson J., Crépin J. Formation and Characterization of Hydride Blisters in Zircaloy-4 Cladding Tubes. *Journal of Nuclear Materials*. 2014. Vol. 449, Iss. 1-3. pp. 132–147.
14. Jeong Y. H., Kim H. G., Kim T. H. Effect of β Phase, Precipitate and Nb-concentration in Matrix on Corrosion and Oxide Characteristics of Zr-xNb Alloys. *Journal of Nuclear Materials*. 2003. Vol. 317, Iss. 1. pp. 1–12.
15. Jeong Y. H., Kim H. G., Kim D. J., Choi B. K., Kim J. H. Influence of Nb Concentration in the α -matrix on the Corrosion Behavior of Zr-xNb Binary Alloys. *Journal of Nuclear Materials*. 2003. Vol. 323, Iss. 1. pp. 72–80.
16. Motta A. T., Couet A., Comstock R. J. Corrosion of Zirconium Alloys Used for Nuclear Fuel Cladding. *Annual Review of Materials Research*. 2015. Vol. 45, Iss. 1. pp. 311–343.
17. Singh R. N., Kishore R., Sinha T. K., Kashyap B. P. Hydride Blister Formation in Zr-2.5wt%Nb Pressure Tube Alloy. *Journal of Nuclear Materials*. 2002. Vol. 301, Iss. 2-3. pp. 153–164.
18. Pierron O. N., Koss D. A., Motta A. T., Chan K. S. The Influence of Hydride Blisters on the Fracture of Zircaloy-4. *Journal of Nuclear Materials*. 2003. Vol. 322, Iss. 1. pp. 21–35.
19. Raynaud P. A., Koss D. A., Motta A. T. Crack Growth in the Through-Thickness Direction of Hydrided Thin-Wall Zircaloy Sheet. *Journal of Nuclear Materials*. 2012. Vol. 420, Iss. 1-3. pp. 69–82.
20. Perryman E. C. W. Pickering Pressure Tube Cracking Experience. *Nuclear Energy*. 1978. Vol. 17, Iss. 2. pp. 95–105.
21. Platonov P. A., Ryazantseva A. V., Saenko G. P. et al. The Study of the Cause of Cracking in Zirconium Alloy Fuel Channel Tubes: Poster Paper. In: *ASTM Zirconium in the Nuclear Industry – 8th International Symposium* (available as AECL report RC-87, 1988).
22. Obukhov A.V. Reactor's Irradiation Effect and Post-Radiation Annealing on the Elemental Composition And Crystal Structure Of The Second Phases In Zirconium Alloys E110 and E635. A Dissertation ... Candidate of Technical Sciences. Ulyanovsk, 2022. 143 p.
23. Shishov V. N. Regularities and Mechanisms of Formation of the Microstructure of Zr – Nb – (Fe – Sn – O) Alloys and its Evolution Under Neutron Irradiation. An Abstract ... Doctor of Technical Sciences. Moscow, 2012. 47 p.
24. Kearns J. J., Woods C. R. Effect of Texture, Grain Size, and Cold Work on the Precipitation of Oriented Hydrides in Zircaloy Tubing and Plate. *Journal of Nuclear Materials*. 1966. Vol. 20, Iss. 3. pp. 241–261.
25. Markelov V. A. Improving the Composition and Structure of Zirconium Alloys to Ensure the Operability of Fuel Rods (TVEL), Fuel Assemblies (TVS) and Pressure Pipes of the Active Zones of Water-Cooled Reactors with Increased Resource and Fuel Burnout. An Abstract ... Doctor of Technical Sciences. Moscow, 2010. 46 p.
26. Coleman C. E. Effect of Texture on Hydride Reorientation and Delayed Hydrogen Cracking in Cold-Worked Zr-2.5Nb. *Zirconium in the Nuclear Industry: 5th Conference*. 1982. pp. 393–411.
27. Kiran Kumar N. A. P., Szpunar J. A., He Z. Preferential Precipitation of Hydrides in Textured Zircaloy-4 Sheets. *Journal of Nuclear Materials*. 2010. Vol. 403, Iss. 1-3. pp. 101–107.
28. Roy C., Jacques J. G. {1017} Hydride Habit Planes in Single Crystal Zirconium. *Journal of Nuclear Materials*. 1969. Vol. 31, Iss. 2. pp. 233–237.
29. Arunachalam V. S., Lentinen B., Östberg G. The Orientation of Zirconium Hydride on Grain Boundaries in Zircaloy-2. *Journal of Nuclear Materials*. 1967. Vol. 21. pp. 241–248.
30. Ambler G. F. R. Grain boundary hydride habit in Zircaloy-2. *Journal of Nuclear Materials*. 1968. Vol. 28, Iss. 3. pp. 237–245.
31. Perovic V., Weatherly G. C., Simpson C. J. Hydride Precipitation in α/β Zirconium Alloys. In: *Perspectives in Hydrogen in Metals: Collected Papers on the Effect of Hydrogen on the Properties of Metals and Alloys*. 1986. pp. 469–479.
32. Perovic V., Weatherly G. C. The Nucleation of Hydrides in a Zr-2.5 wt% Nb Alloy. *Journal of Nuclear Materials*. 1984. Vol. 126. pp. 160–169.
33. Perovic V., Weatherly G. C., MacEwen S. R., Leger M. The influence of Prior Deformation on Hydride Precipitation in Zircaloy. *Acta Metallurgica et Materialia*. 1992. Vol. 40, Iss. 2. pp. 63–372.
34. Yu. Udagawa, Yamaguchi M., Abe H., Sekimura N., Fuketa T. Ab Initio Study on Plane Defects in Zirconium–Hydrogen Solid Solution and Zirconium Hydride. *Acta Materialia*. 2010. Vol. 58, Iss. 11. pp. 3927–3938.
35. Bai J. B., Prioul C., Francois D. Hydride Embrittlement in Zircaloy-4 Plate: Part I. Influence of Microstructure on the Hydride Embrittlement in Zircaloy-4 at 20 °C and 350 °C. *Metallurgical and Materials Transactions: A*. 1994. Vol. 25, Iss. 6. pp. 1185–1197.
36. Bai J.B., JI N., Gilbon D., Prioul C., François D. Hydride Embrittlement in Zircaloy-4 Plate: Part II. Interaction Between the Tensile Stress and the Hydride Morphology. *Metallurgical and Materials Transactions*. 1994. Vol. 25A. pp. 1199–1208.
37. Wang Z., Garbe U., Li H., Wang Y., Studer A. J., Sun G., Harrison R. P., Liao X., Vicente Alvarez M. A., Santisteban J. R., Kong C. Microstructure and Texture Analysis of δ -hydride Precipitation in Zircaloy-4 Materials by Electron Microscopy and Neutron Diffraction. *Journal of Applied Crystallography*. 2014. Vol. 47, Iss. 1. pp. 303–315.
38. Kim Y. S., Perlovich Yu., Isaenkova M., Kim S. S., Cheong Y. M. Precipitation of Keoriented Hydrides and Textural

Change of α -Zirconium Grains During Delayed Hydride Cracking of Zr – 2.5% Nb Pressure Tube. *Journal of Nuclear Materials*. 2001. Vol. 297. pp. 292–302.

39. Kim J. S., Kim S. D., Yoon J. Hydride Formation on Deformation Twin in Zirconium Alloy. *Journal of Nuclear Materials*. 2016. Vol. 482. pp. 88–92.

40. Kiran Kumar N. A. P., Szpunar J. A. EBSD Studies on Microstructure and Crystallographic Orientation of δ -hydrides in Zircaloy-4, Zr – 1% Nb and Zr – 2.5% Nb. *Materials Science and Engineering: A*. 2011. Vol. 528, Iss. 21. pp. 6366–6374.

41. Tenishev A.V. Differential Scanning Calorimetry Determination of the Hydrogen Solubility in E110opt and E635 Zirconium Alloys. *Russian Metallurgy*. 2022. № 6. pp. 1427–1433.

42. Perlovich Yu., Isaenkova M., Fesenko V. Use of Generalized Pole Figures in the X-ray Study of Textured Metal Materials. *Zeitschrift für Kristallographie*. 2007. Iss. 26. pp. 327–332.

43. Perlovich Yu. A., Isaenkova M. G., Krymskaya O. A., Fesenko V. A., Babich Y. A. Optimization of the Procedure for Determining Integral Texture Parameters of Products from Zirconium-Based Alloys Using the Orientation Distribution Function. *IOP Conference Series: Materials Science and Engineering*. 2016. Vol. 130. 012056.

44. MTEX Software for Analyzing and Modeling Crystallographic Textures by Means of EBSD or Pole Figure Data. TU Chemnitz, Germany. URL: <http://mtex-toolbox.github.io/Documentation>. (Accessed: 05.06.2023).

45. LaboTex v. 3.0 by LaboSoft – Krakow, Poland. URL: <http://www.labosoft.com.pl>. (Accessed: 22.05.2023).

46. Lutterotti L., Vasin R., Wenk H.-R. Rietveld Texture Analysis from Synchrotron Diffraction Images. I. Calibration and Basic Analysis. *Powder Diffraction*. 2014. Vol. 29, Iss. 1. pp. 76–84.

47. Wenk H.-R., Lutterotti L., Kaercher P., Kanitpanyacharoen W., Miyagi L., Vasin R. Rietveld Texture Analysis from Synchrotron Diffraction Images. II. Complex Multiphase Materials and Diamond Anvil Cell Experiments. *Powder Diffraction*. 2014. Vol. 29, Iss. 3. pp. 220–232.

48. Isaenkova M. G., Perlovich Yu. A. Regularity of the Development of Crystallographic Texture and Substructural Heterogeneity in Zirconium Alloys During Deformation and Heat Treatment. Moscow: “MEPhI”, 2014. 528 p.

49. Isaenkova M. G., Perlovich Y. A., Fesenko V. A., Krymskaya O. A., Krapivka N. A., Tkhu S. S. Regularities of Recrystallization of Rolled Single Crystals And Polycrystals of Zirconium and Alloy Zr – 1%Nb. *Physics of Metals and Metallography*. 2014. Vol. 115, Iss. 8. pp. 807–815. 